Acta Crystallographica Section A
Foundations of Crystallography
ISSN 0108-7673

Received 26 September 2007
Accepted 23 January 2008

Precise determination of anomalous scattering factors of Ge by using X-ray resonant scattering

Masami Yoshizawa,[a]* ShengMing Zhou,[b] Riichirou Negishi,[a] Tomoe Fukamachi[a] and Takaaki Kawamura[c]

[a]Saitama Institute of Technology, Fusaiji, Fukaya, Saitama 369-0293, Japan, [b]Shanghai Institute of Optics and Fine Mechanics, Chinese Academy of Science, Tacheng Road 295, Jiading, Shanghai, China, and [c]University of Yamanashi, Kofu, Yamanashi 400-8510, Japan. Correspondence e-mail: yoshizaw@sit.ac.jp

Variations of peak position of the rocking curve in the Bragg case are measured from a Ge thin crystal near the *K*-absorption edge. The variations are caused by a phase change of the real part of the atomic scattering factor. Based on the measurement, the values of the real part are determined with an accuracy of better than 1%. The values are the most reliable ones among those reported values so far as they are directly determined from the normal atomic scattering factors.

1. Introduction

Near an absorption edge, the real f' and imaginary f'' parts of the anomalous scattering factor change very remarkably as a function of X-ray energy. The change can be observed not only in the absorption coefficient but also in the intensities of the diffracted and transmitted beams. As the energy of X-rays from synchrotron radiation can be tuned to a specified value, it is possible to measure the shape of rocking curves or the intensities of the diffracted and transmitted beams at the specified energy. The change of the imaginary part f'' has been used to study crystal structures of magnetic materials because the intensity of X-ray magnetic scattering is enhanced by f'' (Namikawa *et al.*, 1985). A ferro-type orbital ordering in ruthenium oxide has been observed recently (Kubota *et al.*, 2005) based on the fact that the anomalous scattering factor can be a tensor near an absorption edge. It is well known that the large change of the anomalous scattering factor is useful to determine the phase of a crystal structure factor (Materlik *et al.*, 1994). If we have more precise values of anomalous scattering factors near the absorption edge, phase determination should be much improved. As the anomalous scattering factors in a crystal are different from those for an isolated atom, it is necessary to use the anomalous scattering factors of the crystal for the phase determination.

In this paper, we report precise determination of the real part of the anomalous scattering factor by comparing peak positions of the transmitted and diffracted rocking curves against the incident angle. We take a Ge crystal as an example. The obtained values are most reliable among those studied so far. In order to evaluate the previously reported values, the obtained values are compared with the values calculated by Sasaki (1989) using the method of Cromer & Liberman (1970), those determined by using the dispersion relation (Kawamura & Fukamachi, 1978), and those by using the semicircular behavior of the atomic scattering factor f (Yoshizawa *et al.*, 2005).

2. Change of rocking curves due to anomalous scattering factor

The atomic scattering factor is given by

$$f = f^0 + f' + if'' = |f| \exp(i\theta), \tag{1}$$

where f^0 is the normal atomic scattering factor. The phase θ is given by

$$\theta = \tan^{-1} k_f, \tag{2}$$

with

$$k_f = f''/(f^0 + f'). \tag{3}$$

Since the imaginary part f'' is always positive or equal to 0 ($f'' \geq 0$), θ varies between 0 and π. By the linear absorption coefficient μ, f'' is expressed as

$$f'' = \left(\frac{c\omega}{4\pi}\right)\mu, \tag{4}$$

where c is the light velocity and ω is X-ray energy.

The Fourier coefficient χ_h of X-ray polarizability is expressed as

$$\chi_h = \chi_{hr} + i\chi_{hi} = |\chi_{hr}| \exp(i\alpha_{hr}) + i|\chi_{hi}| \exp(i\alpha_{hi}), \tag{5}$$

where

$$\chi_{hr} = -\frac{4\pi}{V\omega^2} \sum_j (f_j^0 + f_j') \exp(i\mathbf{h} \cdot \mathbf{r}_j)\Theta_j, \tag{6a}$$

$$\chi_{hi} = -\frac{4\pi}{V\omega^2} \sum_j f_j'' \exp(i\mathbf{h} \cdot \mathbf{r}_j)\Theta_j. \tag{6b}$$

The atomic units ($\hbar = e = m = 1$) are used. V is the unit-cell volume of the crystal, $\mathbf{h}$ the reciprocal-lattice vector, $\mathbf{r}_j$ the

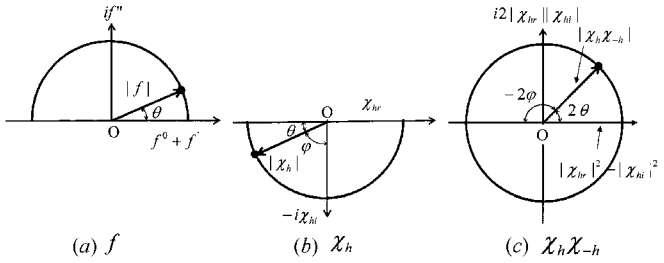

Figure 1
(*a*) Variations of f and its phase, (*b*) those of χ_h and (*c*) those of $\chi_h\chi_{-h}$ for a monoatomic crystal.

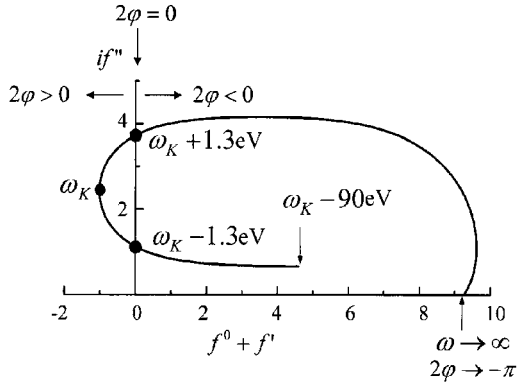

Figure 2
Locus of the atomic scattering factor f of Ge 844 reflection in the complex plane.

position vector of atom j, Θ_j the temperature correction factor for atom j.

As a monoatomic crystal such as Ge has a center of symmetry, χ_{hr} and χ_{hi} are both real and the relation $\chi_h = \chi_{-h}$ holds. Equation (5) can be rewritten as

$$\chi_h = |\chi_h| \exp[i(\alpha_{hr} + \theta)]. \tag{7}$$

Here $\pi \leq \alpha_{hr} + \theta \leq 2\pi$ because $\chi_{hi} \leq 0$, and θ can be written as $\theta = \tan^{-1} k$ with

$$k = \chi_{hi}/\chi_{hr}. \tag{8}$$

If we put

$$\varphi = \frac{\pi}{2} - \theta, \tag{9}$$

$\chi_h\chi_{-h}$ is expressed as

$$\chi_h\chi_{-h} = |\chi_h|^2 \exp(i2\theta) = -|\chi_h|^2 \exp(-i2\varphi). \tag{10}$$

Fig. 1 shows the variations of f, χ_h, $\chi_h\chi_{-h}$ and their phases for a monoatomic crystal. When $\chi_{hi} \neq 0$ and $\chi_{hr} = 0$, $2\theta = \pi$ and $2\varphi = 0$. The condition $2\varphi = 0$ means

$$f^0 + f' = 0. \tag{11}$$

Using this relation, the value of f' can be determined from only f^0 at this condition.

Fig. 2 shows the locus of f in the complex plane with $f^0 + f'$ as the abscissa and f'' as the ordinate for Ge 844 reflection around the K-absorption edge. The anomalous scattering factors are calculated by using the formula based on an

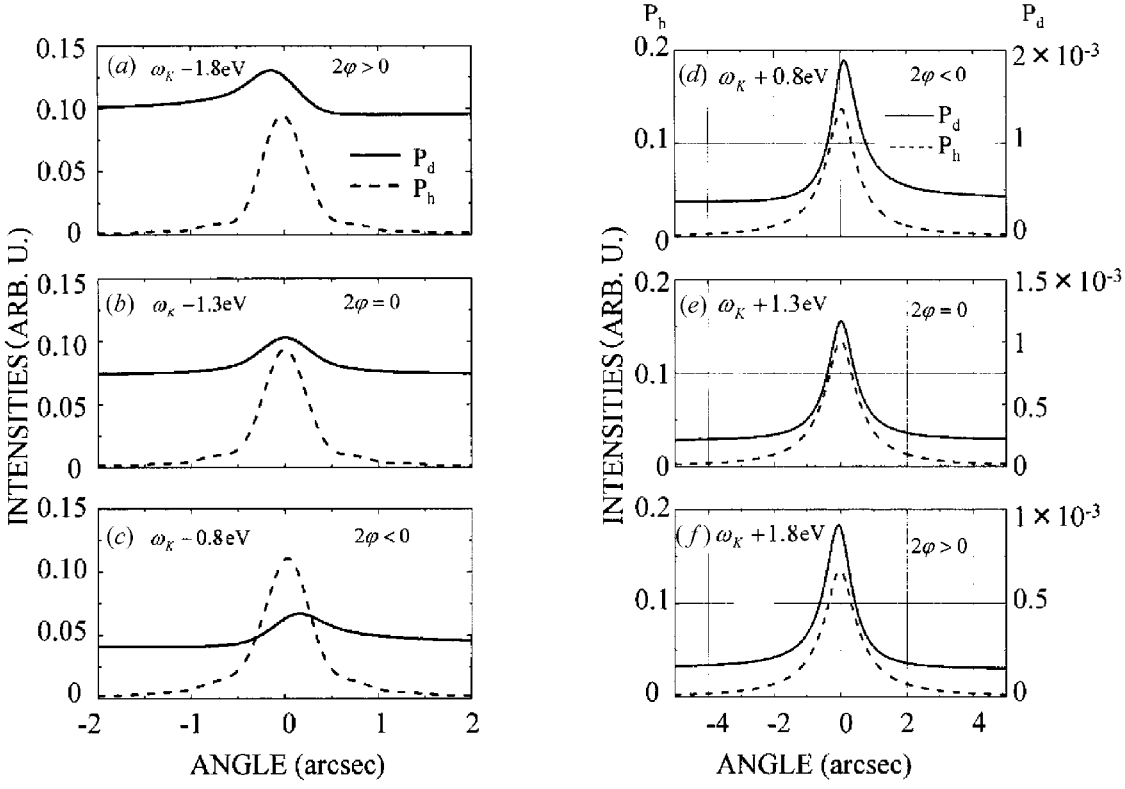

Figure 3
The calculated Ge 844 rocking curves in the Bragg case around the K-absorption edge. (*a*)–(*c*) are those below the edge and (*d*)–(*f*) those above it. The dashed lines show the diffracted curves and the solid lines the transmitted ones.

isolated-atom model of Parratt & Hempstead (1954) with the oscillator strength by Cromer (1965). The correction of life time at the absorption edge is made. Very near the Ge K-absorption edge ω_K, the phase 2φ changes sign. 2φ is negative ($f^0 + f' > 0$) when the X-ray energy ω satisfies either $\omega < \omega_K - 1.3$ eV or $\omega > \omega_K + 1.3$ eV, and it is positive ($f^0 + f' < 0$) when $\omega_K - 1.3 < \omega < \omega_K + 1.3$ eV. The condition $2\varphi = 0$ is satisfied when $\omega = \omega_K \pm 1.3$ eV.

Figs. 3(*a*)–(*c*) show the calculated rocking curves for Ge 844 reflection in the Bragg case at energies just below the absorption edge by using the resonant X-ray dynamical theory (Fukamachi *et al.*, 2002). The diffracted and transmitted rocking curves are shown for the X-ray energies at $\omega_K - 1.8$ eV (*a*), $\omega_K - 1.3$ eV (*b*) and $\omega_K - 0.8$ eV (*c*), respectively. The thickness of the crystal is 80 μm. Peaks of the diffracted curves (P_h) locate at the Bragg angle (center) and those of the transmitted curves (P_d) move around the Bragg angle as seen in Figs. 3(*a*)–(*c*). The FWHM of the rocking curve is approximately 0.6 arcsec. As seen in Fig. 3(*a*), the peak of the transmitted curve locates at a lower angle from that of the diffracted curve. The intensities on the left side of P_d are higher than those on the right side. The opposite variations are observed in Fig. 3(*c*) compared to those in Fig. 3(*a*). In Fig. 3(*b*), the peak positions of the diffracted and transmitted curves coincide, and the heights of the left and the right sides of P_d are the same. Figs. 3(*d*)–(*f*) show the diffracted and transmitted rocking curves which are calculated for the X-ray energies above the absorption edge at $\omega_K + 0.8$ eV (*d*), $\omega_K + 1.3$ eV (*e*) and $\omega_K + 1.8$ eV (*f*). The thickness of the sample is 60 μm. The transmitted peak locates slightly at the high-angle side of the Bragg condition in Fig. 3(*d*) and at the low-angle side in Fig. 3(*f*); the variations are opposite to those in Figs. 3(*a*) and 3(*c*). The FWHM of the peak increases to 1.6 arcsec. The transmitted intensity is

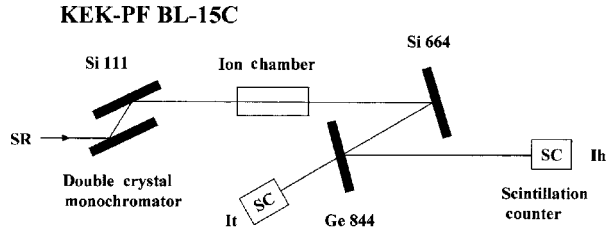

Figure 4
Schematic diagram of the measuring system of rocking curves in the present experiment.

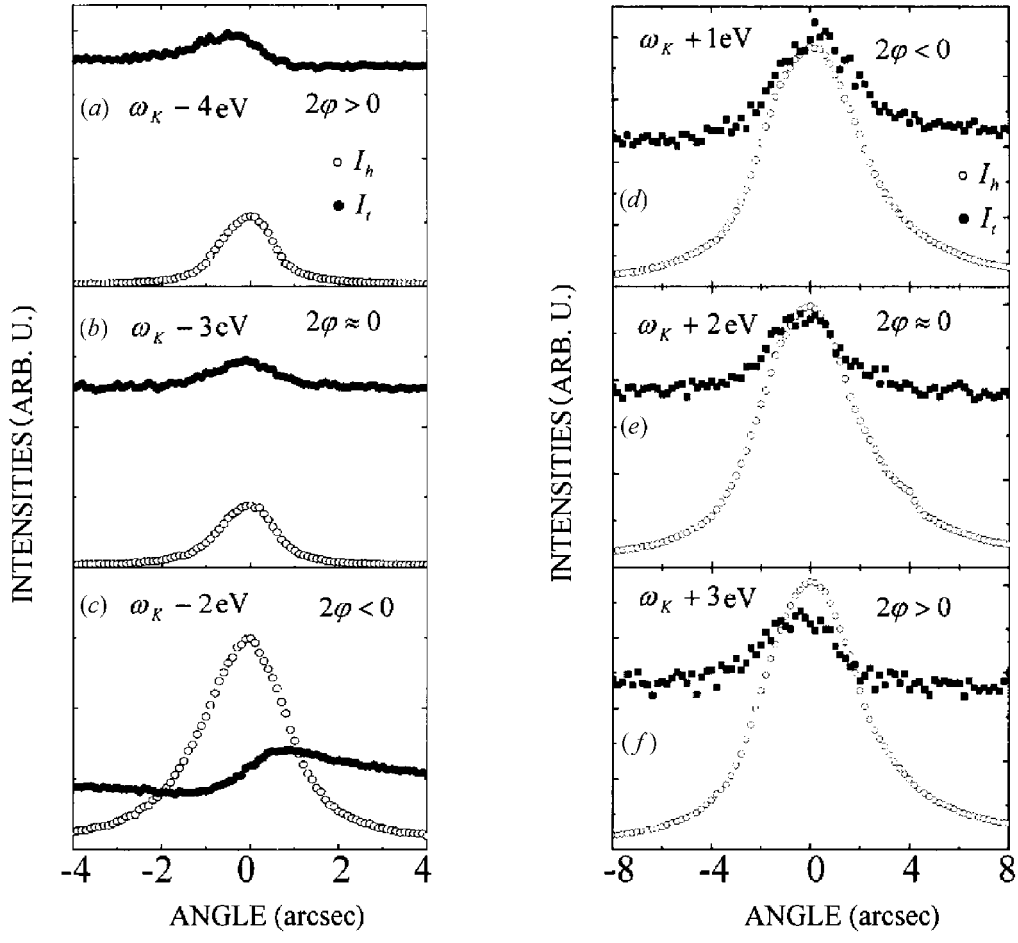

Figure 5
The measured Ge 844 rocking curves in the Bragg case around the K-absorption edge. (*a*)–(*c*) are those below the edge and (*d*)–(*f*) those above it. The open circles show the diffracted curves and the filled circles the transmitted ones. The sample thickness is 80 μm for (*a*)–(*c*) and 60 μm for (*d*)–(*f*).

Table 1
f'_{Ge} values by the present experiment (present), by the isolated-atom model (CLS), by using the dispersion relation (DR) and by using the semicircular behavior (SC).

The differences are estimated by using the relation $\sum |f'_{other} - f'_{present}| / \sum |f'_{present}|$, where $f'_{present}$ are those determined by the present experiment and f'_{other} are the values by CLS, DR or SC, respectively.

Refl.	Energy (eV)	f'_{Ge} (Present)	f'_{Ge} (CLS)	f'_{Ge} (DR)	f'_{Ge} (SC)
844	$\omega_K - 3.0 \pm 0.5$	−9.24	−7.99	−9.08	−9.22
840	$\omega_K - 1.30 \pm 0.5$	−10.21	−8.89	−10.06	−10.01
555	$\omega_K - 1.0 \pm 0.5$	−10.58	−9.10	−10.23	−10.16
660	$\omega_K - 1.0 \pm 0.5$	−10.83	−9.10	−10.23	−10.16
555	$\omega_K - 1.0 \pm 0.5$	−10.58	−9.36	−10.62	−10.70
840	$\omega_K - 1.5 \pm 0.5$	−10.21	−8.92	−10.28	−10.35
844	$\omega_K - 2.0 \pm 0.5$	−9.24	−8.52	−9.66	9.72
Errors (%)			12.6	2.5	2.9

approximately two orders of magnitude weaker than the diffracted one and the transmitted curves show distinct change in shape. The transmitted peak locates at the higher-angle side than the diffracted one, and the intensities on the high-angle side are stronger than those on the low-angle side as seen in Fig. 3(*d*). The opposite variation is seen in Fig. 3(*f*) as compared to Fig. 3(*d*). The peak positions of the diffracted and transmitted curves coincide and the intensities on both sides of each curve in Fig. 3(*e*) are approximately the same. Thus we can judge whether the condition $2\varphi = 0$ is satisfied or not by measuring the peak positions as well as the symmetry of the transmitted rocking curves with respect to those of the diffracted curves. At the condition $f^0 + f' = 0$, the value of f' can be determined only from f^0. Because f^0 is calculated theoretically with an accuracy better than 1% in a reflection

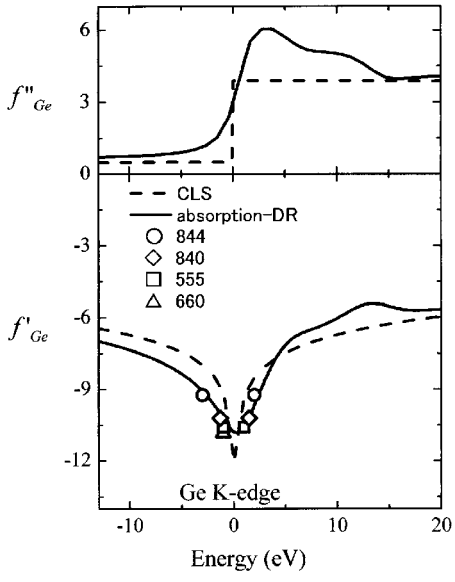

Figure 6
The anomalous scattering factors f' (lower figure) and f'' (upper figure) of Ge. Open circles, diamonds and squares represent f' values obtained by using 844, 840 and 555 reflections, respectively. The triangle represents f' using the 660 reflection. The solid curve for f'' represents the values determined by measuring the absorption coefficient and the solid curve for f' those determined by using DR. The dashed curves represent f' and f'' calculated by the CLS method.

case with high Miller index, it is an advantage of the present approach that f' can be obtained with an error of less than 1%. Then the f' values determined are the most reliable ones among the values reported previously.

3. Experimental results

A schematic diagram of the measuring system is shown in Fig. 4. The experiment was carried out at beamline 15C at KEK-PF. The X-rays from synchrotron radiation were monochromated by using an Si 111 double-crystal monochromator and an Si 664 monochromator. The energy of the X-rays was calibrated by measuring XANES from a thin Ge plate (27 µm) according to the quantitative criterion of the Ge *K*-absorption edge (ω_K = 11 103 eV) with an accuracy of ±0.5 eV.

Fig. 5 shows a series of measured rocking curves for several X-ray energies near the Ge *K*-absorption edge. Figs. 5(*a*)–(*c*) show the diffracted (open circles) and transmitted (filled circles) rocking curves measured at 4 eV (*a*), 3 eV (*b*) and 2 eV (*c*) below the absorption edge, respectively. Figs. 5(*d*)–(*f*) show those at 1 eV (*d*), 2 eV (*e*) and 3 eV (*f*) above the absorption edge, respectively. The angle of each rocking curve is adjusted to have the peak of the diffracted curve locate at zero. The peak of the transmitted curve locates at the lower-angle side compared to that of the diffracted beam in Fig. 5(*a*) and the intensities on the low-angle side are higher than those on the high-angle side. In Fig. 5(*b*), the peak positions of the transmitted and the diffracted curves are approximately the same. In Fig. 5(*c*), the peak of the transmitted curve locates at the higher-angle side of the peak of the diffracted beam and the intensities at 4 arcsec are higher than those at −4 arcsec. By comparing the above results with the calculated ones in Fig. 3, it is clear that $f^0 + f' = 0$ is satisfied at $\omega_K - 3$ eV. On the other hand, the variations in Figs. 5(*d*)–(*f*) are different from those in Figs. 5(*a*)–(*c*). The transmitted peak locates at the higher-angle side to the diffracted peak in Fig. 5(*d*), and the intensities at +8 arcsec are higher than those at −8 arcsec. The locations of the transmitted and diffracted peaks are approximately the same in Fig. 5(*e*). In Fig. 5(*f*), the transmitted peak locates at the lower-angle side compared to the diffracted one, and the intensities at −8 arcsec are higher than those at +8 arcsec. This means that the condition $f^0 + f' = 0$ is satisfied at 2 eV above the absorption edge. By changing the reflection indices to 660, 555 and 840 and repeating similar processes, we obtained f' values of Ge. The values and the corresponding X-ray energies are shown in Table 1 and Fig. 6.

4. Discussion

As the accuracy of the determined values in the present experiment is estimated to be better than 1%, we should evaluate the accuracy of the previously reported values. In Table 1, f' values of Ge obtained in the present experiment are shown together with those calculated based on the isolated-atom model (CLS), those obtained by using the dispersion relation (DR) and those obtained by using the semicircular

behavior of f (SC). In Fig. 6, these f' (lower figure) values are plotted together with f'' (upper figure). The f' values obtained by SC and DR are quoted from Yoshizawa *et al.* (2005). The f' values of CLS are calculated by Sasaki (1989) using the Cromer & Liberman (1970) method. The bottom row of Table 1 shows the percentages of difference between the present experimental values and the values determined by the other methods. The average differences in the values of CLS, DR and SC from the values of the present experiment are 12.6, 2.5 and 2.8%, respectively. The largest difference between the present values and those by CLS can be understood by the fact that the electron state in the conduction band of the crystal is very different from the free-electron state in an isolated atom. If the anomalous scattering factor in the crystal is calculated by using a first-principles many-body theory (Fujikawa *et al.*, 2004), the difference should become much smaller. The results of DR and SC show excellent agreement with the present results. Errors in the result of DR come from inhomogeneous thickness of the sample and the errors in the X-ray energy when the absorption coefficient is measured. Those in the results of SC come from the height and the position of a peak just above the absorption edge.

When we obtain the value of the structure factor $|F|$ from the *Pendellösung* fringe, we must measure the thickness of the sample with high precision and make the temperature correction. In the present approach for a monoatomic crystal, however, neither precise measurement of thickness nor the temperature correction is needed, which is an advantage of the present approach. On the other hand, the present approach can be applied to limited cases as the number of reflections available is limited. The present approach can be used for other purposes. For example, in the energy correction of the crystal monochromator by using the shape of the absorption edge, it is difficult to improve the accuracy by more than ± 0.5 eV due to the natural width of the spectrum. If the X-ray energy at the condition $2\varphi = 0$ is determined very accurately, the energy correction of the monochromator should be improved.

In the above, we have treated the Bragg case, but we can also treat the Laue case in a similar way. In a biatomic crystal such as GaAs, the condition of $2\theta = 0$ which corresponds to $\chi_{hi} = 0$ can be used as shown by Negishi *et al.* (1998, 2004, 2007).

The authors are particularly indebted to Professor Masayasu Tokonami of Saitama Institute of Technology for his valuable discussions, and are deeply grateful to Dr Keiichi Hirano of KEK-PF and Dr Isao Matsumoto of Wako System Laboratory for help in experiments during this study. This work was carried out under the approval of the Program Advisory Committee of PF (Proposal No. 2000G046, 2003G211, 2004G234 and 2006G274). This work was partly supported by the 'High-Tech Research Center' Project for Universities: matching found subsidy from MEXT, 1999–2003 and 2004–2007.

References

Cromer, D. T. (1965). *Acta Cryst.* **18**, 17–23.
Cromer, D. T. & Liberman, J. (1970). *J. Chem. Phys.* **53**, 1891–1898.
Fujikawa, T., Konishi, T. & Fukamachi, T. (2004). *J. Electron Spectrosc.* **196**, 195–206.
Fukamachi, T., Negishi, R., Zhou, S., Yoshizawa, M. & Kawamura, T. (2002). *Acta Cryst.* A**58**, 552–558.
Kawamura, T. & Fukamachi, T. (1978). *Jpn. J. Appl. Phys.* **17**, Suppl. 17-2, 224–226.
Kubota, M., Murakami, Y., Mizumaki, M., Ohsumi, H., Ikeda, N., Nakatsuji, S., Fukazawa, H. & Maeno, Y. (2005). *Phys. Rev. Lett.* **95**, 26401.
Materlik, G., Sparks, C. J. & Fischer, K. (1994). *Resonanant Anomalous X-ray Scattering.* Amsterdam: Elsevier Science.
Namikawa, K., Ando, M., Nakajima, T. & Kawata, H. (1985). *J. Phys. Soc. Jpn*, **54**, 4099–4102.
Negishi, R., Fukamachi, T., Yoshizawa, M., Hirano, K. & Kawamura, T. (2007). *Phys. Status Solidi A*, **204**, 2694–2699.
Negishi, R., Fukamachi, T., Yoshizawa, M., Zhou, S., Xu, Z., Kawamura, T., Matsumoto, I., Sakamaki, T. & Nakajima, T. (1998). *J. Appl. Cryst.* **31**, 351–355.
Negishi, R., Yoshizawa, M., Zhou, S., Matsumoto, I., Fukamachi, T. & Kawamura, T. (2004). *J. Synchrotron Rad.* **11**, 266–271.
Parratt, L. G. & Hempstead, C. F. (1954). *Phys. Rev.* **94**, 1593–1600.
Sasaki, S. (1989). KEK Report 88-14, pp. 1–136.
Yoshizawa, M., Zhou, S., Negishi, R., Fukamachi, T. & Kawamura, T. (2005). *Acta Cryst.* A**61**, 553–556.